Nuclear spin polarization in single self-assembled $In_{0.3}Ga_{0.7}As$ quantum dots by electrical spin injection

Pablo Asshoff, Gunter Wüst, and Andreas Merz
Institut für Angewandte Physik and DFG Center for Functional Nanostructures (CFN), Karlsruhe Institute of Technology (KIT), D-76131 Karlsruhe, Germany

Dimitri Litvinov and Dagmar Gerthsen
Laboratorium für Elektronenmikroskopie and CFN, Karlsruhe Institute of Technology (KIT), D-76131 Karlsruhe, Germany

Heinz Kalt and Michael Hetterich
Institut für Angewandte Physik and CFN, Karlsruhe Institute of Technology (KIT), D-76131 Karlsruhe, Germany
(Received 8 April 2011; published 6 September 2011)

For a single $In_{0.3}Ga_{0.7}As$ quantum dot in a spin light-emitting diode, we compare the nuclear spin polarization created by a spin polarized electrical current with the nuclear spin polarization originating from optically generated spin polarized carriers. As detection method we employ high-resolution optical spectroscopy of the Overhauser shift. We find that optically and electrically generated electron spin populations in the quantum dot result in a nuclear spin polarization of comparable magnitude, provided the injected electrons have the same spin polarization degree in both excitation modes. An asymmetric dependence of nuclear spin polarization on electron spin polarization is observed, consistent with the theoretical treatment. The results imply that nuclear spin polarization degrees of ∼58% can be achieved by purely electrical means in self-assembled quantum dots.

DOI: 10.1103/PhysRevB.84.125302 PACS number(s): 78.67.Hc, 72.25.Hg, 33.35.+r, 72.25.Dc

I. INTRODUCTION

For quantum information processing (QIP), the spin-split electron subbands in a semiconductor quantum dot (QD) constitute a physical realization of a two-level system. Confinement of the electron states is achieved either by limiting the physical extension of the surrounding material[1] (self-assembled QDs) or by electrical fields[2] (electrostatic QDs). Electrons with well-defined spin states can be injected into these QDs using optical and electrical schemes.[3–5] Recently, much work was devoted to the question how the injected spin-polarized electrons interact with the nuclear spins of the QD.[5–17] In particular, extensive research has been carried out on nuclear spin polarization via optical injection into self-assembled QDs and electrical injection into electrostatically defined double QDs.[10] These efforts have been mainly driven by the relevance of the hyperfine interaction to quantum computation schemes. It provides a pathway to access the nuclear spins for applications in a nuclear spin-based QIP.[6,18] On the other hand, spin polarization of the nuclei resulting from the hyperfine interaction with the electron spins poses an obstacle to applications of QDs in QIP schemes based on the electron spin, since flip-flop processes limit the coherence time of the electron spins.[7,9,10]

In this paper, a system allowing for both electrical and optical spin injection in self-assembled $In_{0.3}Ga_{0.7}As$ QDs is analyzed. The magnitude of nuclear spin polarization for these injection modes is determined. Is is shown that efficient polarization of the nuclei can be achieved, independent of the injection process. The system investigated is a spin light-emitting diode[19,20] (spin-LED) with incorporated self-assembled QDs,[4] subject to an externally applied magnetic field $\mathbf{B}_0$. Nuclear spin polarization in single $In_{0.3}Ga_{0.7}As$ QDs is quantified by detecting the Overhauser shift δ_s, which is due to the effective magnetic field $\mathbf{B}_N$ associated with the aligned nuclear spins.[21] This magnetic nuclear field $\mathbf{B}_N$ acts similarly as the externally applied field $\mathbf{B}_0$,[8,9] resulting in a total effective magnetic field of magnitude $\mathbf{B}_0 \pm \mathbf{B}_N$. The Overhauser shift δ_s and the effective nuclear field in the reference direction $B_{N,z}$ are related via $\delta_s = -\mu_B g B_{N,z}$, where g is the g-factor of the electron experiencing the effective nuclear field and μ_B the Bohr magneton.

II. SAMPLE AND EXPERIMENT

The sample used for the experiment is sketched in Fig. 1. Fabrication and processing of the sample were carried out as follows: A GaAs:Zn(001) wafer ($p \sim 1 \times 10^{19}$ cm^{-3}) was used as substrate. On the substrate a ∼500-nm layer of GaAs:Be ($p \sim 1 \times 10^{19}$ cm^{-3}) was grown using a III–V molecular-beam epitaxy (MBE) facility, followed by 100 nm i-GaAs, the $In_xGa_{1-x}As$ QDs/wetting layer (WL) (see Ref. 22 for details) and a 25-nm-thick i-GaAs spacer. From optical characterization it was found that the QDs have a negligible in-plane asymmetry. The heterostructure was then transferred to a second MBE facility, designed for the growth of II–VI materials, where 750 nm of the spin aligner material $Zn_{0.95}Mn_{0.05}Se$:Cl ($n \sim 10^{18}$ cm^{-3}) followed by a 200-nm-layer of ZnSe:Cl ($n = 5 \times 10^{18}$ cm^{-3}) were deposited. The latter layer improves the ohmic contact to the subsequently evaporated In contact pad. Then, a thin gold layer was thermally evaporated wherein apertures were defined by electron beam lithography. Finally, optical lithography was employed to define square-shaped spin-LEDs, one of which with a surface area of $(400\ \mu\text{m})^2$ is investigated here.

Complementary structural information was gathered with electron microscopy methods on a reference sample. Plan-view transmission electron microscopy (TEM) revealed a QD sheet density of $\sim 5 \times 10^{10}$ cm^{-2}. An overview cross-section TEM image and the composition evaluation of an enlarged section

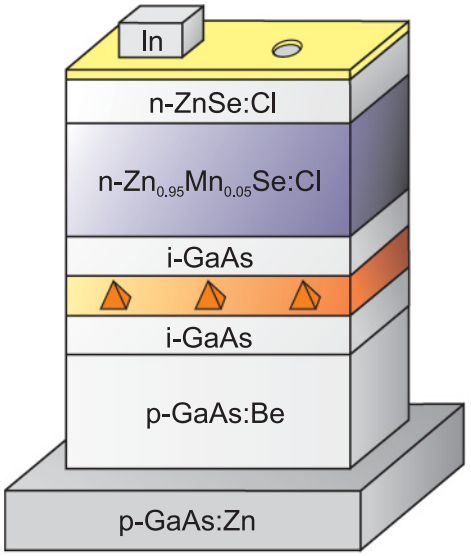

FIG. 1. (Color online) Cross-sectional schematical view (not to scale) of the spin-LED. In the $In_xGa_{1-x}As$ QDs, spin populations are created by either electrical operation or optical excitation. The gold mask on top of the structure, which contains the apertures, is indicated.

by lattice fringe analysis (CELFA)[23] are shown in Fig. 2. In the CELFA image the local In concentration in a typical $In_xGa_{1-x}As$ QD is displayed. It amounts to $x \simeq 30\%$ at the center of the dot.

The spin polarization degree of the QD nuclei during electrical and optical excitation was determined using the spectroscopic setup displayed in Fig. 3. The sample was placed on piezoelectric actuators in a magneto-optical cryostat at a temperature $T = 5$ K and with a field $\mathbf{B_0}$ applied in Faraday geometry. To investigate a single QD, one of the gold apertures on top of the spin-LED was positioned in the focus of a 60× microscope objective mounted inside the cryostat, providing an optical path between the sample

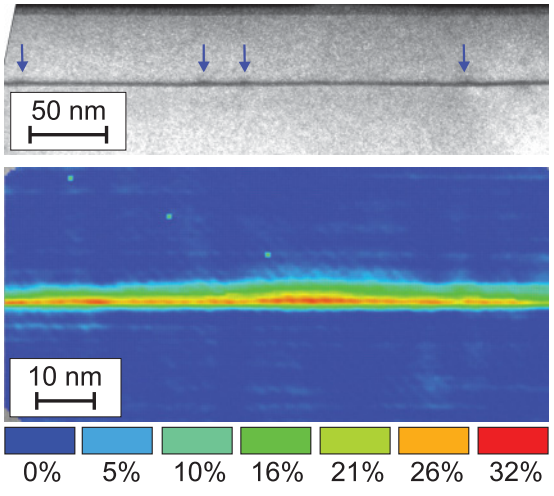

FIG. 2. (Color online) (002) dark-field TEM and CELFA images of the QD type investigated. In the top TEM image, arrows indicate the position of larger QDs. The local In concentration x in the environment of an $In_xGa_{1-x}As$ QD is revealed in the CELFA image.

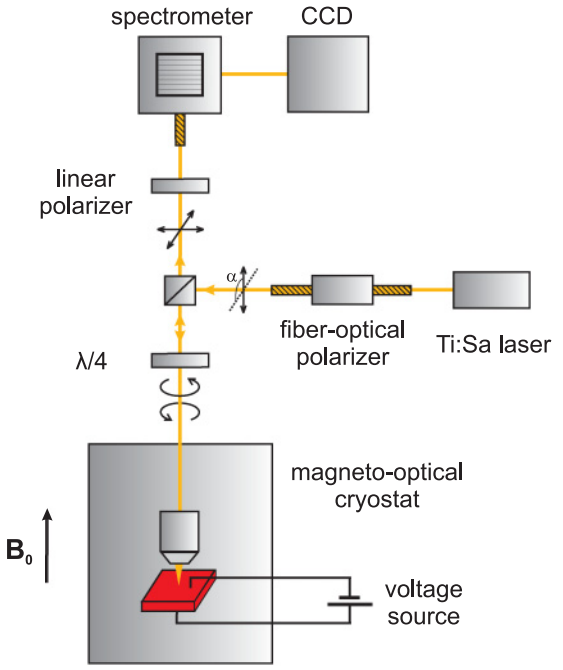

FIG. 3. (Color online) Experimental setup. The magneto-optical cryostat contains the sample located beneath a microscope objective. Fibers are indicated as hatched lines. The lower right branch is used for photoexcitation only.

surface and the outside of the cryostat, used for detection and laser excitation. Light emitted by the sample during either electrical or optical excitation was collected by the microscope objective. Outside the cryostat, the collected light traversed a quarter-wave plate followed by a Glan-Thompson polarizer. These optics allowed us to determine the circular polarization degree (P_C) of the emitted light, which indicates the electron spin polarization inside the QD[1] and is defined as $P_C = (I_{\sigma^+} - I_{\sigma^-})/(I_{\sigma^+} + I_{\sigma^-})$, with $I_{\sigma^{+(-)}}$ denoting the intensity of $\sigma^{+(-)}$-polarized light. The light was then fed to a double spectrometer with two 1200 grooves/mm gratings through a graded-index multimode fiber. With a charge-coupled device the spectrally dispersed light was detected, using an acquisition time of 20 s per spectrum. A high spectral resolution (16 μeV per pixel further enhanced by the applied fitting procedure) was achieved, which is crucial for revealing the Overhauser shift δ_s.

For the electroluminescence (EL) measurements, a voltage was applied across the heterostructure. Electrons were injected from the top In contact pad, traversed the $Zn_{0.95}Mn_{0.05}Se$:Cl layer, and left it with a defined spin polarization due to the giant Zeeman splitting of the material in the applied field $\mathbf{B_0}$.[1,19] The spin polarized electrons were then injected into the $In_{0.3}Ga_{0.7}As$ QDs sandwiched between thin GaAs layers, which renders a suitable band structure for the injection process. The injection efficiency highly depends on the individual QD investigated.[24] Unpolarized holes were flowing into the QDs and the WL from the bottom part of the spin-LED, leading to radiative recombination.

In the case of the photoluminescence (PL) experiments, photons at an energy of 1.42 eV from a continuous-wave Ti:sapphire laser were guided by a fiber to the cryostat. An all-fiber Babinet-Soleil compensator was used to adjust the

phase between the light components propagating in the fiber such that the light left the fiber linearly polarized and at an angle of choice α. The beam was collimated and propagated through a quarter-wave plate, whereby its polarization state was altered. By tuning the Babinet-Soleil compensator and changing the angle at which linearly polarized light was incident the quarter-wave plate, purely σ^+- and σ^--polarized light could be created, as well as both polarization states at a desired ratio. This fiber-based polarization controller prevents any artifacts resulting from beam walk-off effects that would inevitably occur when optical components are rotated. Light with a selected polarization state then impinged on the sample and excited electron-hole pairs in the WL. By changing the helicity of the exciting light, populations with different spin polarizations in the WL were generated. The electrons and holes relaxed into the QDs and recombined, leading to light emission.

III. RESULTS AND DISCUSSION

A representative illustration of acquired spectra is given in Fig. 4. The data were obtained at $T = 5$ K and at $B = 6$ T. For an individual QD, the Zeeman-split emission lines are shown for electrical excitation as well as for linearly, σ^+- and σ^--polarized photoexcitation. Two spectra were recorded for each excitation condition, with the detection setup being sensitive only to either σ^+- or σ^--polarized light. In the graph, dashed lines indicate the energies at which QD emission occurs during linearly polarized photoexcitation. In this excitation configuration, the emission lines have the same intensities $I_{\sigma^{+(-)}}$, corresponding to a zero net electron spin polarization. Considering emission during σ^+- or σ^--polarized excitation, it can be clearly seen that an additional splitting between the spin sublevels arises, originating from the nuclear field. This Overhauser shift results from a net spin polarization of the optically generated electrons (corresponding to emission lines with unlike intensities), which causes a transfer of electron spin to the nuclei via flip-flop processes. The nuclear magnetic field can be determined by comparing the absolute splitting between the spin sublevels. For electrical excitation, the spectrum is slightly red shifted, which is attributed to Joule heating.

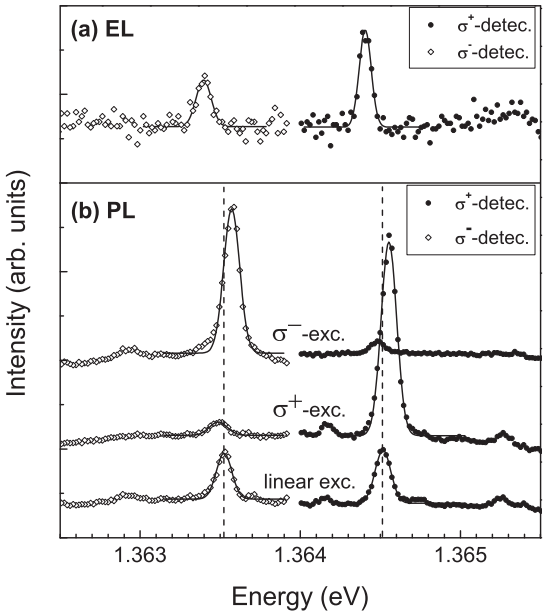

FIG. 4. Zeeman-split emission lines ($B = 6$ T, $T = 5$ K) from an individual QD for (a) electroluminescence (EL) and (b) photoluminescence (PL) with Gaussian line-shape fits (solid lines).

Spin polarization of the nuclei in two single QDs is discussed in more detail. In QD A, a positively charged exciton (X^+) interacts with the nuclei, the X^+ transition is centered at 1.3598 eV. In QD B, hyperfine interaction is mediated by neutral excitons (X^0), the excitonic emission is centered at 1.3608 eV. The exciton types were determined by fine structure measurements[25] and from the power-dependent behavior of the emission intensities.[26] Nuclear spin polarization in the dots depends primarily on two factors: the spin polarization degree of the injected electrons and excitation power. With increasing excitation power, nuclear spin alignment exhibits a saturation behavior.[11]

First, the Overhauser shift $\delta_{s,\max} = 2\sum_k x_k A_k I_k$ for a fully polarized nuclear spin system is calculated, where x_k, A_k, and I_k is the relative abundance, hyperfine constant, and nuclear spin of element k (In, Ga, As), respectively.[12] As for the strong applied magnetic fields, it can be assumed that the wave function is strongly confined,[27] and the local element concentrations at the center of the dot ($x_{\mathrm{In}} = 0.15$, $x_{\mathrm{Ga}} = 0.35$, $x_{\mathrm{As}} = 0.50$) are relevant for $\delta_{s,\max}$. Using reference values for A_k and I_k from Ref. 28, the maximum Overhauser shift then calculates to $\delta_{s,\max} = 189$ μeV.

To investigate the saturation behavior of the nuclear spin system during continuous electrical spin injection into the QDs, the excitation current was gradually increased, starting from a depolarized state. When the current was adjusted, 2 min were provided for the nuclear spin bath to equilibrate.[29] The saturation behavior of QD A is shown in Fig. 5 for $B = 2$ T and $B = 4$ T. Similarly as reported for optical spin injection, the Overhauser shift rises nonlinearly and saturates with increasing excitation power. At $B = 2$ T, the Overhauser shift amounts to $\sim$24 μeV in saturation and reaches $\sim$60 μeV at $B = 4$ T. This corresponds to a nuclear spin polarization degree of 13% and 32%, respectively. A pronounced dependence of the circular polarization degree P_C on excitation current can be seen at $B = 4$ T, while at $B = 2$ T its value remains almost constant. The saturation behavior of QD B is shown in Fig. 6. At $B = 2$ T, an Overhauser shift of $\sim$110 μeV is observed. This corresponds to a nuclear spin polarization degree of 58%, which is among the highest observed at $B = 2$ T and almost twice as high as P_C.

In Figs. 5 and 6, along with the saturation behavior, the circular polarization degree P_C of the recombining electrons is shown. For electrical excitation, the spin polarization degree is intrinsically linked to the external magnetic field. In this case, spin polarization of the electrons is determined by the spin polarization efficiency of the paramagnetic diluted magnetic semiconductor and spin scattering processes during transport to the QDs.[30] In addition, electron spin polarization depends on the current density, due to effects such as increased scattering rates and state filling in the structure.[30,31] This results in the observed drop of the electron spin polarization degree with increasing excitation power, in contrast to the increase of nuclear spin polarization.

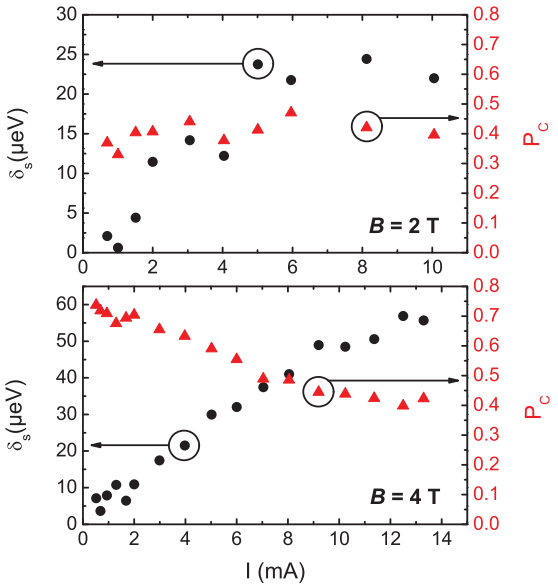

FIG. 5. (Color online) Saturation behavior of the Overhauser shift δ_s (black dots) and circular polarization degree P_C (red triangles) for QD A as function of the current through the spin-LED. Results for $B = 2$ T and $B = 4$ T are shown.

Similar saturation measurements were done for photoexcitation. A high excitation power was chosen to saturate the nuclear spin system. Then, in contrast to electrical excitation, the net spin polarization degree of the optically generated carriers could be varied at the specified magnetic field by adjusting the polarization of the impinging light. When the polarization was changed, 5 min were provided before spectra were recorded. For QD A, the Overhauser shift is plotted against the circular polarization degree P_C of emitted photons in Fig. 7 (red dots). Results for $B = 2$ T and $B = 4$ T are displayed. In addition, data points obtained from the electroluminescence experiments were included (black diamonds). These data points correspond to the Overhauser shift achieved at the highest currents applied to the device, when the system was close to saturation. From the graph, it can be clearly seen that electrical spin injection results in a similar nuclear spin polarization as optical excitation, provided that the circular polarization degree P_C is of the same magnitude.

Furthermore, an asymmetric dependence of the Overhauser shift on P_C exists, with higher nuclear spin polarization

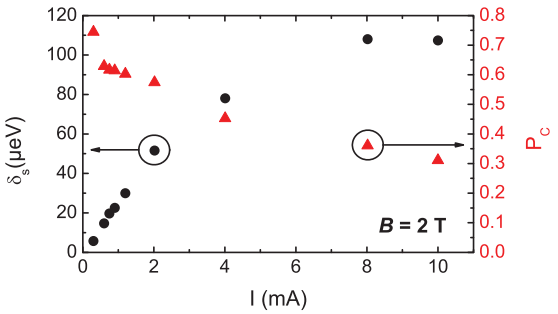

FIG. 6. (Color online) Saturation behavior of the Overhauser shift δ_s (black dots) and circular polarization degree P_C (red triangles) for QD B as function of the current through the spin-LED, $B = 2$ T.

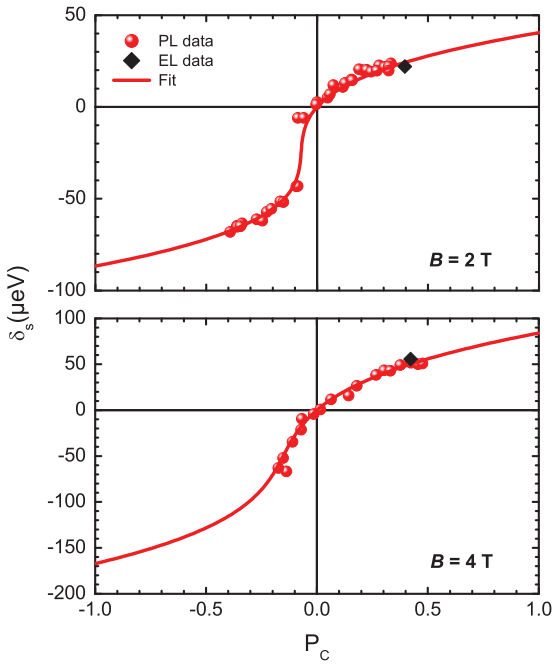

FIG. 7. (Color online) Overhauser shift δ_s plotted against the circular polarization degree P_C of QD A for magnetic fields $B = 2$ T and $B = 4$ T. Results from optical excitation (electrical excitation) are shown as red dots (black diamonds). The lines are fits to the photoluminescence data using the described theoretical model.

degrees obtained at negative values of P_C. From this asymmetrical shape, parameters characteristic of the system can be derived by a fitting procedure. A theoretical model used before in Refs. 12–16 is employed. In the model, the contact hyperfine interaction term is treated as a time-dependent perturbation to the motion of the electron spin in a magnetic field.[32] Nuclear polarization arises due to flip-flop processes mediated by the hyperfine interaction.[10] If electrons of a certain spin polarization prevail, these processes are efficiently polarizing the nuclei in the dot. In contrast, spin diffusion out of the dot results in nuclear depolarization, e.g., by dipole-dipole interactions with neighboring nuclei. During continuous excitation, both nuclear polarization and depolarization take place. The average spin polarization of the nuclei $\langle I_z \rangle$ in the steady state can be obtained by using a rate equation model for the dynamic nuclear polarization:

$$\frac{d\langle I_z\rangle}{dt} = -\frac{1}{T_e}(\langle I_z\rangle - \tilde{Q}\langle S_z\rangle) - \frac{1}{T_d}\langle I_z\rangle, \qquad (1)$$

where T_e is the nuclear spin polarization time and T_d is a time constant characterizing nuclear spin diffusion out of the dot. $\langle S_z \rangle$ is the average electron spin polarization, determined experimentally via P_C according to $\langle S_z\rangle = -P_C/2$. $\tilde{Q}$ is a conversion factor relating the electron spin state and the nuclear spin system. It is given by $\tilde{Q} = \sum_j x_j I^j(I^j+1)/S(S+1)$, being derived from the electron spin S and the weighted average of the nuclear spins I^j of the isotopes j according to their relative abundance x_j. In the steady state, the Overhauser shift δ_s is then given by the implicit expression

$$\delta_s = -\frac{2\tilde{A}\tilde{Q}\langle S_z\rangle}{1+\frac{T_e(\delta_s)}{T_d}} \qquad (2)$$

with

$$\frac{1}{T_e} = \left(\frac{\tilde{A}}{N\hbar}\right)^2 \frac{2 f_e \tau_c}{1 + \left(\frac{\delta_e + \delta_s}{\hbar}\tau_c\right)^2}. \quad (3)$$

In the calculation, a homogeneous electron wave function $\psi(\mathbf{r}) = \sqrt{2/N v_0}$ was assumed. $\tilde{A}$ was introduced as the averaged hyperfine constant, and N as the number of nuclei in the QD. The fraction of time the QD is occupied by an electron is f_e, and the electron Zeeman splitting due to the external magnetic field is δ_e. The electron spin correlation time τ_c describes the time the electron spin precesses unperturbed in the nuclear field.[18]

Fits with the model to the data obtained from photoexcitation are displayed in Fig. 7. The asymmetrical shape results from the fact that the nuclear spin polarization time T_e depends on the level spacing $|\delta_e| \pm |\delta_s|$ between the electron spin sublevels, which requires energy-conserving assisting processes for the flip-flop processes to take place.[17] As parameters for the fit $N = 50\,000$, $\tilde{A} = 46$ μeV, $f_e = 0.1$, $\tilde{Q} = 11.5$, and $g = -0.32$ were used, in accordance with reference values.[10,28,33] For the correlation time and nuclear spin diffusion time $\tau_c = 60$ ps and $T_d = 180$ ms at $B = 2$ T, and $\tau_c = 13$ ps and $T_d = 400$ ms at $B = 4$ T were obtained. This means that when the magnetic field is increased, the correlation time decreases, and spin diffusion characterized by T_d is taking place more slowly. A similar inverse relationship for the development of τ_c and T_d with comparable time scales was found in temperature-dependent measurements of the Overhauser shift.[13] Changes of the parameters in the model, especially of τ_c, were attributed to different excitation conditions. Strikingly, data from the EL experiment agree well with the fits, indicating comparable excitation conditions.

More difficult is the situation for polarization of the nuclei involving uncharged excitons, as in QD B. In this case, the electron-hole exchange interaction should have a considerable influence on the hyperfine interaction between electrons and nuclei. Novel phenomena such as dynamic self-polarization of the nuclei could arise.[17] Furthermore, we calculated that the interplay between the exchange interaction energy and the Zeeman energy gives rise to a nonzero nuclear polarization even if the net electron spin polarization is zero. This behavior was also observed experimentally. A comprehensive investigation of these processes exceeds the scope of this contribution. However, as is apparent from Fig. 6, in these systems high nuclear spin polarization degrees of $\sim$58% can be achieved by electrical injection of spin-polarized electrons.

IV. CONCLUSIONS

To conclude, it was demonstrated that efficient nuclear spin polarization in self-assembled QDs can be achieved by purely electrical means. The nuclear spin polarization degree achieved is comparable with that of optical experiments if the injected electrons have the same spin polarization degree. An asymmetrical behavior of nuclear spin polarization was observed and described by a model, in agreement with experimental data from electrical and optical excitation of the system.

ACKNOWLEDGMENTS

This work has been performed within project A2 of the DFG Research Center for Functional Nanostructures (CFN). It has been further funded by a grant from the Ministry of Science, Research and the Arts of Baden-Württemberg (Grant No. 7713.14-300). We acknowledge financial support from the Karlsruhe School of Optics and Photonics (A.M. and P.A.) and the Karlsruhe House of Young Scientists (P.A.).

[1] M. Hetterich, W. Löffler, P. Asshoff, T. Passow, D. Litvinov, D. Gerthsen, and H. Kalt, in *Advances in Solid State Physics*, edited by R. Haug (Springer, Berlin, 2009), Vol. 48, p. 103.

[2] J. M. Elzerman, R. Hanson, L. H. Willems van Beveren, B. Witkamp, L. M. K. Vandersypen, and L. P. Kouwenhoven, Nature **430**, 431 (2004).

[3] M. Atatüre, J. Dreiser, A. Badolato, A. Högele, K. Karrai, and A. Imamoğlu, Science **312**, 551 (2006).

[4] P. Asshoff, A. Merz, H. Kalt, and M. Hetterich, Appl. Phys. Lett. **98**, 112106 (2011).

[5] D. J. Reilly, J. M. Taylor, J. R. Petta, C. M. Marcus, M. P. Hanson, and A. C. Gossard, Science **321**, 817 (2008).

[6] A. Imamoğlu, E. Knill, L. Tian, and P. Zoller, Phys. Rev. Lett. **91**, 017402 (2003).

[7] P.-F. Braun *et al.*, Phys. Rev. Lett. **94**, 116601 (2005).

[8] S. W. Brown, T. A. Kennedy, D. Gammon, and E. S. Snow, Phys. Rev. B **54**, R17339 (1996).

[9] I. A. Merkulov, A. L. Efros, and M. Rosen, Phys. Rev. B **65**, 205309 (2002).

[10] W. A. Coish and J. Baugh, Phys. Status Solidi B **246**, 2203 (2009).

[11] M. N. Makhonin, A. I. Tartakovskii, A. Ebbeens, M. S. Skolnick, A. Russell, V. I. Fal'ko, and M. Hopkinson, Appl. Phys. Lett. **93**, 073113 (2008).

[12] B. Eble, O. Krebs, A. Lemaître, K. Kowalik, A. Kudelski, P. Voisin, B. Urbaszek, X. Marie, and T. Amand, Phys. Rev. B **74**, 081306(R) (2006); B. Eble, Ph.D. thesis, Université Pierre et Marie Curie Paris VI, Paris, 2006.

[13] B. Urbaszek, P.-F. Braun, T. Amand, O. Krebs, T. Belhadj, A. Lemaître, P. Voisin, and X. Marie, Phys. Rev. B **76**, 201301(R) (2007).

[14] P. Maletinsky, C. W. Lai, A. Badolato, and A. Imamoglu, Phys. Rev. B **75**, 035409 (2007).

[15] R. Kaji, S. Adachi, H. Sasakura, and S. Muto, Phys. Rev. B **77**, 115345 (2008).

[16] I. A. Merkulov, Phys. Usp. **45**, 1293 (2002).

[17] V. Korenev, JETP Lett. **70**, 129 (1999).

[18] M. I. D'yakonov and V. I. Perel', in *Optical Orientation*, edited by F. Meier and B. P. Zakharchenya (North-Holland, Amsterdam, 1984).

[19]R. Fiederling, M. Keim, G. Reuscher, W. Ossau, G. Schmidt, A. Waag, and L. W. Molenkamp, Nature **402**, 787 (1999).
[20]M. Holub and P. Bhattacharya, J. Phys. D: Appl. Phys. **40**, R179 (2007).
[21]A. W. Overhauser, Phys. Rev. **92**, 411 (1953).
[22]T. Passow, S. Li, P. Feinäugle, T. Vallaitis, J. Leuthold, D. Litvinov, D. Gerthsen, and M. Hetterich, J. Appl. Phys. **102**, 073511 (2007).
[23]A. Rosenauer and D. Gerthsen, Ultramicroscopy **76**, 49 (1999); A. Rosenauer, Transmission Electron Microscopy of Semiconductor Nanostructures - An Analysis of Composition and Strain (Heidelberg, Springer), Springer Tracts in Modern Physics 182 (2003).
[24]W. Löffler, M. Hetterich, C. Mauser, S. Li, T. Passow, and H. Kalt, Appl. Phys. Lett. **90**, 232105 (2007).
[25]M. Bayer *et al*., Phys. Rev. B **65**, 195315 (2002).
[26]K. Brunner, G. Abstreiter, G. Böhm, G. Tränkle, and G. Weimann, Phys. Rev. Lett. **73**, 1138 (1994).
[27]M.-F. Tsai, H. Lin, C.-H. Lin, S.-D. Lin, S.-Y. Wang, M.-C. Lo, S.-J. Cheng, M.-C. Lee, and W.-H. Chang, Phys. Rev. Lett. **101**, 267402 (2008).
[28]P.-F. Braun, B. Urbaszek, T. Amand, X. Marie, O. Krebs, B. Eble, A. Lemaitre, and P. Voisin, Phys. Rev. B **74**, 245306 (2006).
[29]J. Strand, X. Lou, C. Adelmann, B. D. Schultz, A. F. Isakovic, C. J. Palmstrøm, and P. A. Crowell, Phys. Rev. B **72**, 155308 (2005).
[30]M. Hetterich *et al*., Phys. Status Solidi B **243**, 3812 (2006).
[31]P. Asshoff, W. Löffler, J. Zimmer, H. Füser, H. Flügge, H. Kalt, and M. Hetterich, Appl. Phys. Lett. **95**, 202105 (2009).
[32]A. Abragam, *The Principles of Nuclear Magnetism* (Oxford University Press, Oxford, UK, 2007).
[33]T. Nakaoka, T. Saito, J. Tatebayashi, and Y. Arakawa, Phys. Rev. B **70**, 235337 (2004).